t-J_z ladder: Density-matrix renormalization group and series expansion calculations of the phase diagram

A. Weisse, R. J. Bursill, C. J. Hamer, and Zheng Weihong
School of Physics, The University of New South Wales, Sydney, NSW 2052, Australia
(Received 22 November 2005; published 10 April 2006)

The phase diagram of the two-leg t-J_z ladder is explored, using the density-matrix renormalization group method. Results are obtained for energy gaps, electron density profiles, and correlation functions for the half filled and quarter filled cases. The effective Lagrangian velocity parameter v_ρ is shown to vanish at half filling. The behavior of the one-hole gap in the Nagaoka limit is investigated, and found to disagree with theoretical predictions. A tentative phase diagram is presented, which is quite similar to the full t-J ladder, but scaled up by a factor of about 2 in coupling. Near half filling a Luther-Emery phase is found, which may be expected to show superconducting correlations, while near quarter filling the system appears to be in a Tomonaga-Luttinger phase.

DOI: 10.1103/PhysRevB.73.144508 PACS number(s): 03.70.+k

I. INTRODUCTION

The discovery of high-temperature superconductivity in the cuprate materials has sparked huge interest in models of strongly correlated electrons in low-dimensional systems, such as the Hubbard, t-J and t-J_z models. These models are exactly solvable in one dimension, at least in some special cases; but the two-dimensional models pose a formidable numerical challenge. The "minus sign" problem is a major stumbling block for Monte Carlo calculations in these fermionic systems; and the convergence of density-matrix renormalization group (DMRG) calculations is slow in two dimensions. Exact finite-lattice calculations, though useful, are limited to small lattice sizes; while series expansions have typically only been useful for special cases such as the half filled limit.

In these circumstances, a considerable effort has been invested in the study of "ladder" systems consisting of two or more coupled chains of sites. Ladders provide a "halfway house," in some sense, between one and two dimensions; and they also display some very interesting effects in their own right.[1,2] They display quite different behavior depending on whether the number of legs is even or odd, as in the Haldane effect for the Heisenberg ladders.[3] Furthermore, experimental compounds have been found which form ladders,[4] such as $SrCu_2O_3$,[5] which may allow the theoretical predictions to be tested experimentally.

The t-J model is an "effective Hamiltonian" for the parent Hubbard model, valid when the Coulomb repulsion is large, but nowadays it is considered as an interesting model in its own right.[6,7] The t-J_z model is a variant in which the rotational symmetry is broken, and the spin interactions are Ising-like. The two-leg t-J ladder has been extensively studied, using exact diagonalization,[8–16] quantum Monte Carlo,[17] the DMRG technique,[18–24] a combination of different methods,[25] or using mean-field or approximate analytic methods.[19,26–28] Near half filling, the model has been explored using dimer series expansions.[29–31]

Our object is to study the corresponding two-leg t-J_z ladder, and compare the results for the two models. The t-J_z chain has been discussed by Batista and Ortiz,[32] and the t-J_z model on the square lattice has been treated by several groups.[33–36] Our primary tool is the DMRG approach, supplemented with a few series calculations near half filling.

The phase diagram for the t-J ladder has been discussed by Troyer *et al.*,[10] Hayward and Poilblanc,[12] and Müller and Rice.[14] At large J/t, the holes all clump together, and phase separation occurs into hole-rich and hole-poor regions. At intermediate J/t, near half filling, a "C1S0" or Luther-Emery phase occurs, where the spin excitations are gapped, while there is a gapless charge excitation mode. Troyer *et al.*[10] found evidence of pairing between the holes in this region, together with long-range superconducting correlations with modified d-wave symmetry. The spin gap is discontinuous at half filling, as the simple magnon excitation gives way to a particle-hole excitation with spin. At smaller J/t, the phase structure appears to become more complicated, with a possible C2S2 phase appearing (two gapless charge modes and two gapless spin modes);[14] while at extremely small J/t, a Nagaoka phase is expected to appear,[37] where each hole is surrounded by a region of ferromagnetic spins, forming a ferromagnetic polaron. In that region no spin gap occurs, and the holes repel each other.

The t-J_z ladder might be expected to show similar behavior. The major difference between the models is that quantum spin fluctuations are absent in the t-J_z model, and the system exhibits long-range antiferromagnetic order for half filling at $T=0$, whereas the t-J model does not. This long-range order will be destroyed at any finite temperature, however, and both models will then display similar long-range antiferromagnetic correlations. The two models should be very similar in most other aspects.

This expectation is borne out by our numerical results. The phase diagram for the t-J_z ladder looks very similar to that of the t-J ladder, except that the critical couplings are about twice as large, and the Tomonaga-Luttinger C1S1 phase extends to somewhat higher electron densities.

In Sec. II we specify the model, and consider its behavior in various limiting cases. In Sec. III a brief discussion of the DMRG method is given, and in Sec. IV our numerical results are presented. Our conclusions are given in Sec. V.

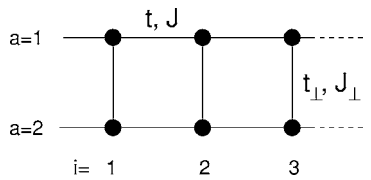

FIG. 1. The *t*-*J* ladder.

II. MODEL

The Hamiltonian of the t-J_z ladder model is (see Fig. 1)

$$H = J\sum_{i,a} S^z_{ia}S^z_{i+1,a} + J_\perp \sum_i S^z_{i1}S^z_{i2} - t\sum_{i,a,\sigma} P(c^\dagger_{ia\sigma}c_{i+1,a\sigma} + \text{H.c.})P - t_\perp \sum_{i,\sigma} P(c^\dagger_{i1\sigma}c_{i2\sigma} + \text{H.c.})P. \quad (1)$$

Here the index $a=1,2$ labels the two legs of the ladder, i labels the rungs of the ladder, the couplings $J, J_\perp$ are the strengths of the spin interactions on legs and rungs, respectively, and $t, t_\perp$ are the hopping strengths on legs and rungs. The projection operators P forbid double occupancy of sites as usual. A density-density interaction term is sometimes included as a relic of the parent Hubbard model, but we do not do that here.

In the half filled case, with a single electron occupying every site ($n=1$), the model becomes equivalent to a simple classical Ising antiferromagnet. The ground state is a doubly degenerate antiferromagnetic state [Fig. 2(a)], with energy

$$E_0 = -\frac{L}{4}(2J + J_\perp), \quad (2)$$

where L is the number of rungs of the ladder. The system can be solved exactly in various limiting cases as follows.

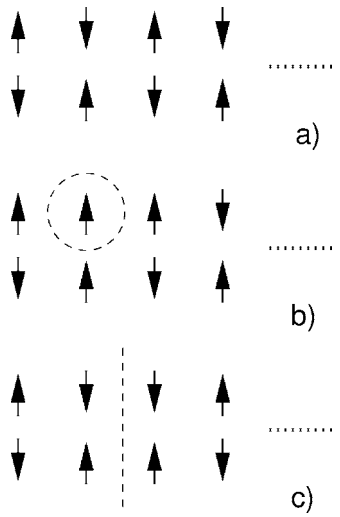

FIG. 2. Spin configurations at 1/2 filling: (a) the antiferromagnetic ground state; (b) an $S^Z=1$ excitation; (c) a domain wall (soliton) excitation.

TABLE I. Rung dimer eigenstates.

Number	Eigenstate	S^z	Energy	
1	$(\|\uparrow\downarrow\rangle - \|\downarrow\uparrow\rangle)/\sqrt{2}$	0	$-J_\perp/4$	singlet
2	$\|\uparrow\uparrow\rangle$	1	$+J_\perp/4$	
3	$(\|\uparrow\downarrow\rangle + \|\downarrow\uparrow\rangle)/\sqrt{2}$	0	$-J_\perp/4$	triplet
4	$\|\downarrow\downarrow\rangle$	−1	$+J_\perp/4$	
5	$\|00\rangle$	0	0	hole-pair singlet
6	$(\|\uparrow 0\rangle + \|0\uparrow\rangle)/\sqrt{2}$	1/2	$-t_\perp$	electron-hole
7	$(\|0\downarrow\rangle + \|\downarrow 0\rangle)/\sqrt{2}$	−1/2	$-t_\perp$	bonding
8	$(\|\uparrow 0\rangle - \|0\uparrow\rangle)/\sqrt{2}$	1/2	$+t_\perp$	electron-hole
9	$(\|0\downarrow\rangle - \|\downarrow 0\rangle)/\sqrt{2}$	−1/2	$+t_\perp$	antibonding

A. Limiting cases

1. Rung dimer limit ($J/J_\perp \to 0, t/J = t_\perp/J_\perp$)

For $J_\perp \gg J$, the system consists of independent dimers on the rungs of the ladder. The eigenstates on a single rung are listed in Table I. The ground state is doubly degenerate here, with both "singlet" and "triplet" states with $S^z=0$ having the same energy, unlike the case of the full t-J ladder. This degeneracy means that one cannot simply compute a perturbation series expansion about the dimer limit in this case, unless one employs degenerate perturbation theory, or introduces an "artificial" interaction to lift the degeneracy.

2. Independent chain limit ($J_\perp/J \to 0, t/J = t_\perp/J_\perp$)

In this case we end up with two independent chains. The chain behavior has been discussed by Batista and Ortiz.[32] They showed that the spins were Neel ordered along the chain in the ground state, which could then be mapped onto an XXZ spin chain. Phase separation occurs at the (rather large) value $J/t=8$ for all hole densities. Below that value, the system forms a gapless Luttinger liquid, with correlation exponent K_ρ and charge velocity v_ρ. The system can be exactly solved via the Bethe ansatz, at quarter filling giving

$$K_\rho = \frac{\pi}{4(\pi-\mu)}, \quad v_\rho = \frac{\pi t \sin\mu}{\mu}, \quad (3)$$

where $\cos\mu = -J/8t$. Thus for $0 \le J/8t \le 1/\sqrt{2}$, we have $1/\sqrt{2} \le K_\rho \le 1$, while for $1/\sqrt{2} \le J/8t \le 1$, we have $K_\rho > 1$, implying that superconducting correlations dominate at large distances. At half filling, on the other hand, we have free fermion (metallic) behavior with $K_\rho = 1/2$.

3. Ising limit ($t/J \to 0, t/J = t_\perp/J_\perp$)

In this limit, the model becomes equivalent to a classical, static Ising model. Unless otherwise stated, we assume periodic boundary conditions, and an even number of rungs L. The ground state at half filling is the fully antiferromagnetic state shown in Fig. 2(a), with $S^z=0$. The low-energy spin excitations will consist either of localized flipped spins ("magnons") with $S^z = \pm 1$, as shown in Fig. 2(b), or else domain wall ("soliton") excitations, as shown in Fig. 2(c), analogous to the "spinon" excitations in Heisenberg chains,

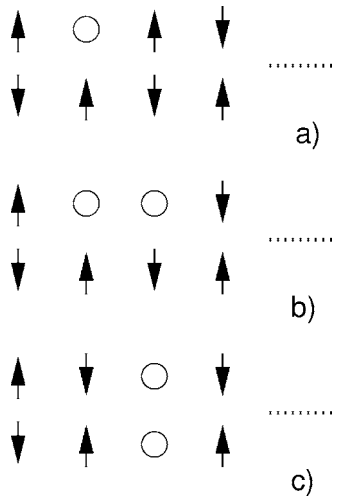

FIG. 3. Charge excitations near to 1/2 filling: (a) a one-hole state; (b), (c) two-hole states.

but carrying $S^z=0$ in this case. The total number of solitons, in the absence of holes, and assuming periodic boundary conditions, has to be even for L even, and odd for L odd, as in the Heisenberg chain. The energy gaps for these two excitations are, respectively,

$$E_{2b} - E_0 = J + \frac{J_\perp}{2},$$

$$E_{2c} - E_0 = J. \tag{4}$$

Since there are no quantum spin fluctuation terms in the Hamiltonian, these spin excitations are of course static, in the absence of holes. Note that since the solitons carry integer spin, there is no possibility of spin-charge separation in this model.

The lowest-energy charge excitation will consist of a single hole in the antiferromagnetic background [Fig. 3(a)], with spin $S^z=\pm 1/2$, and energy

$$E_{3a} - E_0 = \frac{1}{4}(2J + J_\perp). \tag{5}$$

The lowest eigenstates in the two-hole sector consist of a bound pair on adjacent sites [Figs. 3(b) and 3(c)] with spin $S^Z=0$ and energies

$$E_{3b} - E_0 = \frac{1}{4}(3J + 2J_\perp),$$

$$E_{3c} - E_0 = \frac{1}{4}(4J + J_\perp). \tag{6}$$

It is clear that holes will cluster together to minimize the number of "broken bonds" and hence the energy, and the system will be phase separated in this Ising limit.

For small but finite t/J, one can study the system via perturbation series calculations in t/J. Some results of these calculations will be shown in later sections. The single hole states illustrated in Fig. 3(a) are localized states, because there is an energy barrier preventing them from hopping: any hop will disturb the antiferromagnetic alignment of the spins. At higher energy, however, there will be states such as that shown in Fig. 4, with unperturbed energy

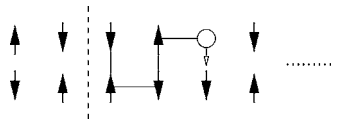

FIG. 4. A hole-plus-domain-wall excitation, showing an allowed zigzag path for hopping (solid line).

$$E_4 - E_0 = \frac{1}{4}(8J + J_\perp), \tag{7}$$

where the hole is free to hop along the zigzag path shown without incurring any further penalty in spin interaction energy. Assuming periodic boundary conditions, these states are made up of a hole plus a soliton for L even, or a hole alone for L odd. For finite t/J, they will form a band of itinerant electron states. The mobility of the electrons in both the chain and the ladder systems is a major point of distinction from the two-dimensional model, where the holes are "confined," i.e., cannot move without creating a "string" of overturned spins behind them, and paying a penalty in spin interaction energy.[38] The states in Figs. 3(a) and 4 will mix as soon as t is turned on, and both configurations should be regarded as hole-soliton bound states.

We will also employ open boundary conditions in our calculations. In this case, the holes will cluster towards the boundaries in the Ising limit, in order to minimize the number of broken bonds. In this case the ground-state energy is

$$E_0 = -\frac{1}{4}[2J(L-1) - LJ_\perp], \tag{8}$$

and the lowest one-hole state [Fig. 5(a)] has energy

$$E_{5a} - E_0 = \frac{1}{4}(J + J_\perp), \tag{9}$$

while the lowest two-hole state [Fig. 5(b)] has energy

$$E_{5b} - E_0 = \frac{1}{4}(2J + J_\perp). \tag{10}$$

The single hole state is not necessarily accompanied by a soliton in this case.

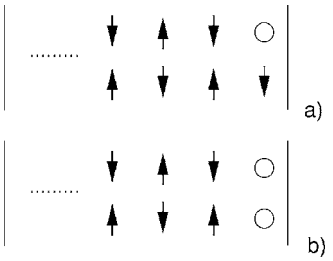

FIG. 5. Charge excitations for the ladder with open boundaries: (a) one hole; (b) two holes.

4. Free-fermion limit ($J/t \to 0, t/J = t_\perp/J_\perp$)

In this limit, a single hole will move through the lattice as a free particle, and its dispersion relation is naively expected to be

$$E_1(k) = -2t\cos k - t_\perp. \tag{11}$$

For simplicity, we shall restrict our remarks henceforth to the isotropic case $t_\perp = t$, when the one-hole energy gap in this limit is $-3t$.

The behavior at small J/t should be similar to that of the t-J model. The one-hole energy in the two-dimensional t-J model has been discussed by a number of authors[33,38–41] At extremely small J/t (of order 10^{-2}, in the region of the Nagaoka phase[37,41]), the hole will be surrounded by a ferromagnetic "polaron," or region of ferromagnetically aligned spins, with spin energy of order JR^2 for a disc of radius R, within which the hole is fully mobile. In this regime, the one-hole energy is

$$E_{1h}/t \sim -4 + c_1\left(\frac{J}{t}\right)^{1/2}, \tag{12}$$

where c_1 is a numerical constant. At larger J/t, however, the lowest-energy states correspond to Brinkman-Rice "string" states,[38,39] where the hole is confined by a string of overturned spins within an antiferromagnetic background. This picture gives a one-hole energy

$$E_{1h}/t \sim -a_1 + b_1\left(\frac{J}{t}\right)^{2/3}, \tag{13}$$

where $a_1 < 4$. Shraiman and Siggia[39] estimated $a_1 = 2\sqrt{3}$ and $b_1 = 2.74$ for the t-J_z model, quite close to the values found numerically by Barnes *et al.*[33] and White and Affleck.[41]

For a one-dimensional chain, no Nagaoka phase occurs, but for a ladder the condition is once again met that holes can hop around closed loops, and a Nagaoka phase is expected.[10] White and Affleck[41] have pointed out that the ferromagnetically aligned spins inside the polaron will orient themselves in the xy plane, rather than along the z axis, because this costs an exchange energy of $J/4$ per bond, rather than $J/2$. For our ladder model, the ferromagnetic "polaron" region will be one dimensional. If the polaron region spans L rungs of the ladder, the cost in magnetic energy will be

$$E_M = \frac{3}{4}JL. \tag{14}$$

Assuming the one-hole wave function to vanish at the edges of the polaron, it will take the form

$$|\psi_k\rangle = A\sum_n \cos(kn)(|n,1\rangle + |n,2\rangle), \quad k = \frac{\pi}{L}, \tag{15}$$

where $|n,a\rangle$ denotes a hole at rung n on leg a of the ladder, and A is a normalization constant. The kinetic or hopping energy is then easily found to be

$$E_K = -3t + t\left(\frac{\pi}{L}\right)^2 \quad (L \to \infty). \tag{16}$$

Minimizing the total energy $E_{1h} = E_M + E_K$ with respect to L we find

$$E_{1h}/t = -3 + \frac{3}{4}\left(\frac{3\pi J}{t}\right)^{2/3} = -3 + 3.35(J/t)^{2/3}. \tag{17}$$

For intermediate J/t, the Brinkman-Rice string picture[38,39] will give a qualitatively similar behavior,

$$E_{1h}/t \sim -a_2 + b_2\left(\frac{J}{t}\right)^{2/3}, \tag{18}$$

where $a_2 < 3$. It is doubtful whether approximations such as those used by Shraiman and Siggia[39] to calculate the coefficients a_2 and b_2 for the two-dimensional (2D) model are at all accurate for the ladder, and we will not attempt an explicit calculation of these coefficients.

B. The effective Hamiltonian

In the regime of physical interest, the t-J ladder is believed to be in a C1S0 or Luther-Emery phase, with gapped spin excitations and gapless charge excitations corresponding to bound hole pairs. Several authors[10,12,22,23] have discussed an effective Hamiltonian to describe these bosonic excitations, which would capture the low-energy physics of the model. Here we merely summarize their results.

In the recent analysis of White, Affleck, and Scalapino,[23] they use a bosonization technique to construct the low-energy effective Hamiltonian

$$H - \mu L = \frac{v_\rho}{2}\int dx\left[K_\rho \Pi_\rho^2 + \frac{1}{K_\rho}\left(\frac{d\theta_\rho}{dx}\right)^2\right], \tag{19}$$

where μ is a chemical potential, Π_ρ is the momentum density conjugate to θ_ρ, v_ρ is the velocity of the corresponding gapless low-energy excitations, and the parameter K_ρ controls the correlation exponents. The two parameters v_ρ and K_ρ must be extracted from numerical data.

White *et al.*[23] show that the finite-size scaling behavior of a general low-energy excitation is

$$E - E_0 = -2p\mu + \frac{2\pi v_\rho}{L}\left(K_\rho m^2 + \frac{p^2}{4K_\rho} + \sum_{k=1}^{\infty} k(n_{Lk} + n_{Rk})\right), \tag{20}$$

where E_0 is the ground-state energy for a given density n, n_{Lk} and n_{Rk} are occupation numbers for left and right moving states of momentum $2\pi k/L$, L is the number of rungs of the ladder, and p and m are integer-valued quantum numbers. The total charge relative to the ground state is $Q = -2p$, and the other quantum number m measures the "'chiral charge."

By measuring the ground-state energies for three different charge states with $\Delta Q = \pm 2$, one can determine the ratio v_ρ/K_ρ:

$$E(p=1)+E(p=-1)-2E_0=\frac{\pi v_\rho}{K_\rho L}. \tag{21}$$

This is directly related to the electron compressibility κ of the two-leg ladder, generally defined as

$$\frac{1}{n^2\kappa}\equiv\frac{1}{2L}\frac{d^2E}{dn^2}=\frac{\pi v_\rho}{2K_\rho} \tag{22}$$

using Eq. (21), where n is the electron density. This formula applies for either periodic or open boundary conditions (BCs), in principle. The velocity may be measured independently using the excitation energy of the lowest state of momentum $2\pi/L$ for periodic BCs,

$$E(n_{R1}=1)-E_0=\frac{2\pi v_\rho}{L}. \tag{23}$$

For open BCs, the momentum spacing is π/L, and the corresponding formula is

$$E(n_1=1)-E_0=\frac{\pi v_\rho}{L}. \tag{24}$$

Hence one can obtain estimates for K_ρ and v_ρ separately.

One may also use "twisted" boundary conditions with the wave function acquiring a phase Φ at the boundary, corresponding to an Aharonov-Bohm flux threading the one-dimensional ring formed by joining the ends of the ladder together. This increases the ground-state energy by

$$E_0\rightarrow E_0+\frac{8\pi v_\rho K_\rho\Phi^2}{L} \tag{25}$$

and allows one to determine the combination $v_\rho K_\rho$. This approach was used by Hayward and Poilblanc.[12]

Finally, White *et al.*[23] discuss how one may estimate K_ρ from the decay of Friedel oscillations in the system. Friedel oscillations are density oscillations produced near the boundary of an open ladder, which decay with a power law corresponding to the exponent K_ρ with distance into the ladder. Using their bosonization analysis and a conformal transformation, White *et al.*[23] show that for a system of length L the density at site (rung) j should vary as

$$\langle n_j\rangle\rightarrow\frac{C\cos(2\pi nj+\beta)}{[(2L/\pi)\sin(\pi j/L)]^{K_\rho}}, \tag{26}$$

where C,β are constants, and $2\pi n$ is the minimum wave vector of Friedel oscillations in the C1S0 phase, corresponding to two holes per wavelength. This is the same wave vector that would occur for a one-component spinless hard core bose gas, made up of tightly bound hole pairs.

Schulz[42] has argued in the case of the t-J ladder that K_ρ should take the universal value $K_\rho=1$ at half filling; but his argument starting from the rung dimer limit is not necessarily applicable to the t-J_z model.

Note that the picture may be complicated by the occurrence of a gapped charge-density wave (CDW) phase at special commensurate filling factors such as $n=0.5$ or $n=0.75$. In this case, the charge-density oscillations persist at all distances from the walls, corresponding to broken translational symmetry and a regular pattern of hole placements. This possibility has been discussed by Riera *et al.*[36] and White *et al.*[23]

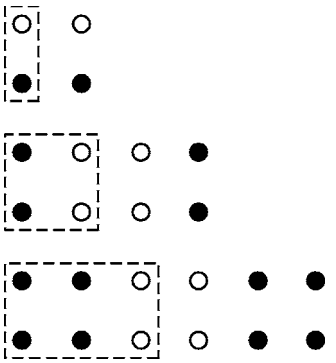

FIG. 6. Infinite lattice construction of the two-leg ladder. Two whole rungs (four sites—open circles) are added per DMRG step. The system and environment blocks increase by one rung (two sites) per DMRG step.

III. METHOD

The model (1) is solved using the density-matrix renormalisation group (DMRG) method.[43] Calculations have been performed at both half filling and quarter filling. Calculations have been performed with both periodic and open boundary conditions (OBCs) in the horizontal direction, but most of the results use OBCs because the convergence is much better in this case.

In the half filled case we have calculated the ground state as well as one-, two-, and four-hole excited states. In the one-hole case we have calculated $S^z=1/2$, 3/2, and 5/2 states. We have calculated energies of these states as well as density profiles $\langle\hat{n}_i\rangle$. The infinite lattice algorithm[43] is employed in this case, using typically $M=60$ states per block and symmetry sector, which corresponds to a total of about 300 system block states. The lattice buildup phase is illustrated in Fig. 6. By running tests for a number of different values of M, we established that the energies of these states have been resolved with sufficiently high accuracy for our purposes.[44]

In the quarter filled case, it is necessary to use the finite lattice method[43] in order to achieve reasonably converged energies. We use the infinite lattice method to build a ladder to a given size, increasing the system block size by a whole rung at each DMRG step as in Fig. 6. We then perform a finite lattice sweep at the fixed lattice size, using the previously developed system blocks to improve the accuracy of the calculation. Once a target size has been completed with a finite lattice sweep, the infinite lattice algorithm is resumed to proceed to a larger target lattice size whereupon the sweeping procedure is again employed. This way we obtain accurate finite lattice method results for a number of lattice sizes, e.g., $N=4$, 8, 12, 16, 24, 32, 64, 128, 256 lattice sites. We found that one finite lattice sweep at each target lattice size was sufficient with subsequent sweeps at the same lattice size adding little improvement compared with increasing the basis size. Wherever necessary, the data are extrapolated

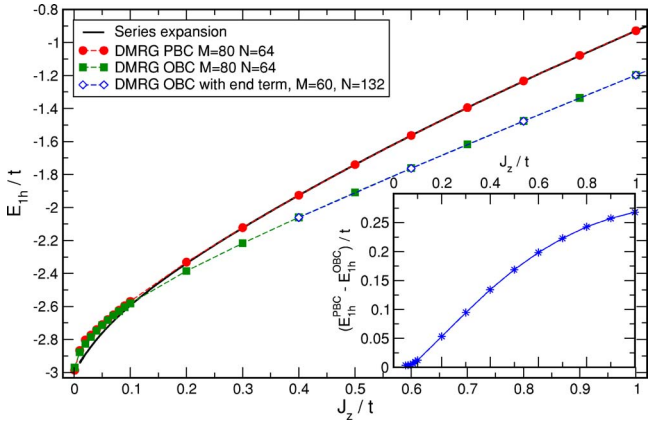

FIG. 7. (Color online) The energy gap $E_{1h}/t=(E_1-E_0)/t$ for one hole, as a function of J_z/t. Filled circles, open boundary conditions; open squares, periodic boundary conditions; solid line, estimates from Ising series expansion.

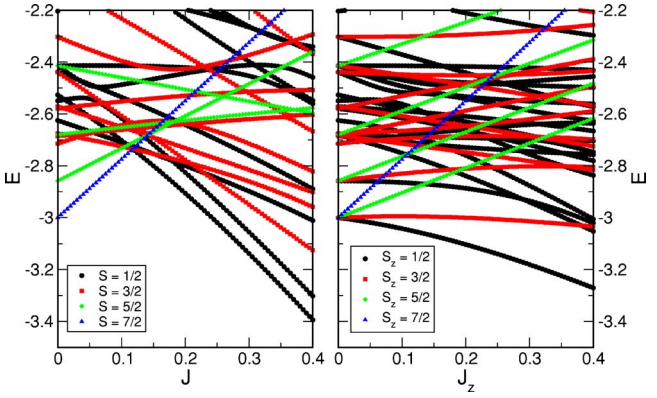

FIG. 8. (Color online) Low-energy spectrum of the t-J (left) and t-J_z (right) model on a four-rung ladder with seven electrons, with different colors used for different total spins.

to the bulk limit $N\to\infty$ by fitting a low-order polynomial in $1/N$ to the finite lattice data.

Typical discarded weights used at the middle of the sweep are around 10^{-6}, where we have used around 300–400 basis states in the system block ($M=60$). However, larger scale calculations, with around 1600 basis states ($M=200$) and discarded weights of around 10^{-8} were used to check that the DMRG convergence was adequate relative to other errors such as finite-size scaling extrapolation errors in difficult cases.

IV. RESULTS

We have calculated numerical DMRG results for this model for the isotropic case, $J=J_\perp\equiv J_z, t=t_\perp$, and for various J_z/t, on lattices of L rungs with L even. Our discussion henceforth will be limited to this case.

A. Near half filling

We begin by considering states with a finite number of holes doped into the half filled system ($n=1$).

1. Single-hole states

Figure 7 shows DMRG estimates of the energy gap for a single hole with spin $S^z=1/2$, as a function of J_z/t, for both periodic and open boundary conditions. The results of a series calculation are also shown for the periodic case. The series estimates were obtained assuming the Nagaoka form (17)

$$f(t)\equiv E_{1h}+3t\sim bt^{1/3}\quad \text{as } t\to 0. \tag{27}$$

Accordingly, the series in t for $f(t)$ was Euler transformed $z=t/(1+t)$ to bring the singularity to $z=1$; then a further change of variable was made,

$$1-\delta=(1-z)^{1/3}, \tag{28}$$

so that one may treat the function $(1-\delta)f(\delta)$ as analytic in δ near $\delta=1$; and finally, differential approximants were used to extrapolate this function to $\delta=1$. It can be seen that the series results agree very well with the DMRG results for $J-z/t>0.3$, but run a little lower below that.

It can also be seen that there is a difference between the DMRG results with periodic and open boundary conditions. As discussed in Sec. II A 3, this is because the state with periodic boundary conditions is actually a hole-soliton bound state. The difference between the two energies is shown in the inset to Fig. 7.

At smaller J_z/t, one is tempted to look for a transition to a Nagaoka phase,[37] i.e., a phase with ferromagnetic spin order or at least a ferromagnetic polaron bubble around the hole. In the t-J_z model, however, the situation is rather different from the t-J model, where the full spin-rotation symmetry applies. The scenario is illustrated in Fig. 8, where we show the complete one-hole energy spectrum of the t-J and t-J_z models on a four-rung cluster. The left-hand panel shows the t-J case, where at $J=0$ the ground state has maximal spin $S=7/2$ (ferromagnetic). As J increases, at some critical coupling J_c this state crosses another state with minimal spin $S=1/2$, which becomes the ground state thereafter. The right-hand panel shows the t-J_z case. At $J_z=0$, the system is rotation symmetric, the Nagaoka theorem applies and the ground state again has the maximal possible spin $S_{\max}$ and degeneracy $2S_{\max}+1$. As soon as J_z becomes finite, however, the symmetry is broken, the multiplet splits into its S^z components, and the state with minimal $S^z=\pm 1/2$ becomes the ground state. Clearly, there is no level crossover in the t-J_z case. All we can expect for increasing J_z is a continuous fading-out of the ferromagnetic correlations. This accords with the smooth approach of the one-hole energy to -3 as $J_z\to 0$ in Fig. 7.

A comparison of the numerical data at small J_z/t with the theoretical prediction (17) gives the following results. A Dlog Pade analysis of the series gives a rather inaccurate estimate of the exponent in the range 0.5–0.7, which would be consistent with 2/3. A fit to the DMRG data over the range 0–0.1, however, gives

$$\frac{E_{1h}}{t}=-3+1.444\left(\frac{J_z}{t}\right)^{0.53}, \tag{29}$$

with an exponent much closer to 1/2 than 2/3. This is illustrated by the difference between the DMRG data and the

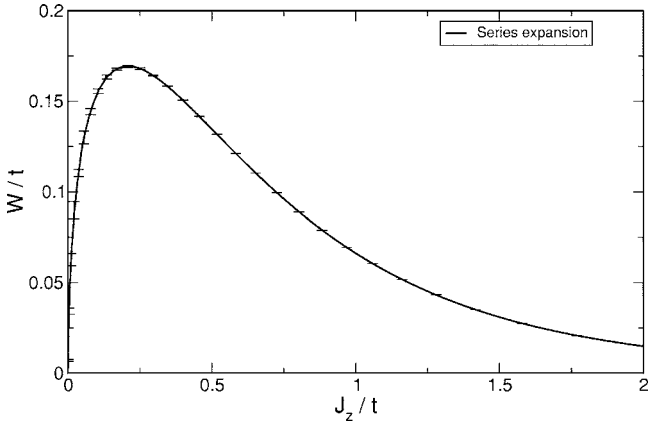

FIG. 9. The one-hole bandwidth W/t as a function of J_z/t, estimated from the Ising series expansion.

series extrapolation in Fig. 7 at small J_z/t. Thus the data do not seem to behave in accordance with theoretical expectations in this instance.

Figure 9 shows the bandwidth for the one-hole state with $S^z=1/2$ predicted by the Ising series expansion, as a function of J_z/t. We see that the predicted bandwidth rises as J_z/t decreases, as one might expect, until at $J_z/t\simeq 0.3$ it reaches a peak, and begins to drop towards zero. Similar behavior in the region of small J/t has been predicted for the two-dimensional (2D) t-J model by Martinez and Horsch[45] and Liu and Manousakis,[46] and confirmed by series calculations.[47] The theoretical predictions assume long-range antiferromagnetic order, and construct an effective Hamiltonian in which the spin dynamics are treated in linear spin-wave theory, and the holes are treated as spinless fermions, following Schmitt-Rink, Varma, and Ruckenstein.[48] The results are consistent with the string picture of Brinkman and Rice,[38] and appear to show a sequence of narrow string excitation peaks in the spectral function, corresponding to holes bound in a linear potential. The effects are even more marked in the t-J_z model.

It would be very interesting to check the actual behavior of the bandwidth by means of DMRG estimates, but unfortunately our codes cannot distinguish different momentum eigenstates.

2. Two-hole states

In studying two- and four-hole states and looking for the phase separation boundary, we wanted to avoid the holes sticking to the boundary and thus obscuring the bulk physics. Accordingly, we have added an extra "boundary potential" term at the sites adjacent to the boundary:

$$H_B = -\frac{J_z}{4}\sum_{i,\sigma} c^{\dagger}_{i,\sigma}c_{i,\sigma}. \tag{30}$$

As it turns out, this makes a negligible difference to the energy gaps in the region of interest. This has been checked in terms of calculations in the absence of a boundary term and with periodic boundary conditions.

In the two-hole sector, the first quantity of interest is the two-hole binding energy

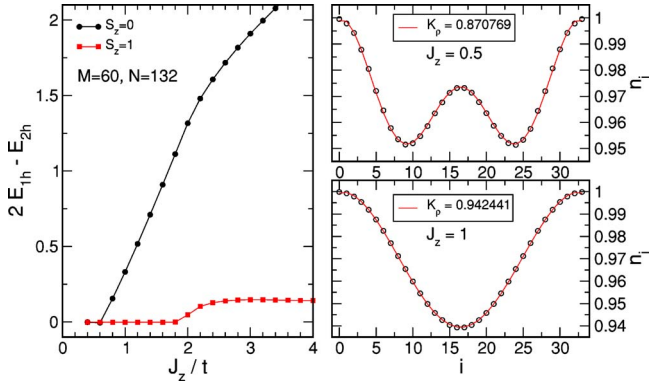

FIG. 10. (Color online) Left: Two-hole binding energies as a function of J_z/t, calculated with OBC and finite boundary potentials. Filled circles: $S^z=0$: filled squares: $S^z=1$. Right: Average electron number per rung as a function of distance along the ladder, for two-hole states on a lattice of 34 rungs: (a) $J_z/t=0.5$; (b) $J_z/t=1.0$. The lines are fits using Eq. (32).

$$E_B = 2E_1 - E_2 - E_0. \tag{31}$$

Figure 10 shows the binding energy as a function of J_z/t for both $S^z=0$ and $S^z=1$, computed with open boundary conditions. It can be seen that a two-hole bound state with $S^z=0$ forms for large J_z/t, but the binding energy vanishes at $J_z/t\simeq 0.60$, and below this point the holes do not bind. In the $S^z=1$ channel, there is a small binding energy at large J_z/t, which vanishes at $J_z/t\simeq 1.8$.

Similar results have been found for other members of this family of models. For the 2D t-J_z model, Riera and Dagotto[34] estimated that the holes become unbound at $J_z/t\simeq 0.18$; while for the t-J ladder, Jurecka and Brenig[31] suggest that hole binding vanishes at $J/t\simeq 0.5$. There is binding in the $S=1$ channel for the t-J ladder, but it is considerably smaller than in the $S=0$ channel.

Wherever the two-hole binding energy is positive, we expect a continuous band of two-hole bound states to appear above the ground state; so that within the two-hole sector, particle-hole excitations (excitons) can occur down to zero energy. In other words, excitons with $S^z=0$ are gapless, as found by Troyer *et al.*[10] for the t-J ladder.

We note that the spin energy gap between the $S^z=1$ and $S^z=0$ two-hole states also drops to zero at $J_z/t=0.6$. It always remains below the $S^z=1$ magnon energy $3J/2$; or in other words, an exciton with $S^z=1$ in the two-hole sector has an energy substantially below that of the magnon. Therefore the spin gap drops discontinuously as one moves away from half filling, which again agrees with the behavior found by Troyer *et al.*[10] for the t-J ladder.

The right panels of Fig. 10 show profiles of the electron density in the two-hole state as a function of distance along the ladder, calculated for a lattice of 34 rungs with open boundary conditions. At low J_z/t, the two holes are unbound and separated from each other, forming two distinct troughs in the density profile (Fig. 10). At $J_z/t\simeq 0.6$ a sharp crossover takes place, where the two holes bind together and form a single trough in the density profile. As it happens, both

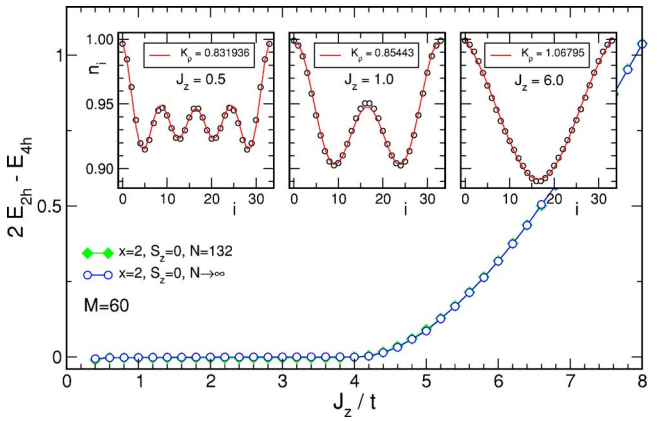

FIG. 11. (Color online) Four-hole binding energy as a function of J_z/t, calculated with OBC and finite boundary potentials. Insets: Electron density profiles at characteristic values of J_z/t, together with fits to the corresponding Friedel expression.

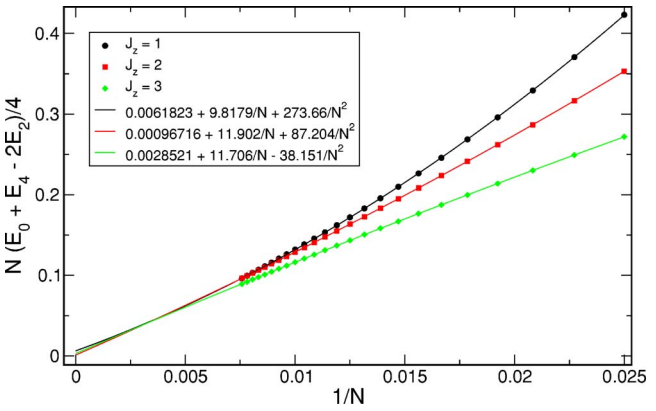

FIG. 12. (Color online) Four-hole binding energy as a function of $1/N=1/(2L)$, at $J_z/t=1$, 2, and 3.

profiles can be fitted quite well with a Friedel oscillation form

$$\langle n_j \rangle = c_0 + \frac{c_1 \sin[2\pi(n+1/2)j/(L+1)]}{\{(L+1)\sin[\pi j/(L+1)]\}^{K_\rho}}, \tag{32}$$

where $n=2$ and $K_\rho=0.87$ in case (a) and $n=1$ and $K_\rho=0.92$ in case (b).

3. Four-hole states

The four-hole binding energy for $S^z=0$ is shown as a function of J_z/t in Fig. 11. We have checked that it is finite at large J_z/t, and vanishes smoothly at $J_z/t \simeq 4$. This is taken to mark the point where phase separation occurs. The smooth behavior of the binding energy may indicate a Kosterlitz-Thouless transition at this point. The insets show examples of the electron-density profiles as functions of distance along the ladder for the four-hole ground state. For $J_z/t=0.5$, we see four separated holes; for $J_z/t=1.0$, we see two separated hole pairs; and for $J_z/t=6.0$, we see a single four-hole cluster, reinforcing the picture given above. Note that the Friedel form (32)) again fits the density profiles remarkably well, upon choosing the appropriate value for n. The fits in the pair binding region indicate that the parameter K_ρ lies approximately in the range 0.8–1.0 near half filling.

Next, we attempt to measure the isothermal compressibility in the non-phase-separated region, whose inverse is

$$\kappa^{-1} = n^2 N[E_4 + E_0 - 2E_2]/4, \tag{33}$$

where $N=2L$ is the number of sites, and $n=(N-2)/N$ the electron density. Figure 12 shows $\kappa^{-1}n^{-2}$ as a function of $1/N$, for some couplings $J_z/t<4$, fitted by a quadratic polynomial in $1/N$. The extrapolations to the bulk limit $N\to\infty$ are compatible with zero, indicating that the inverse compressibility vanishes at half filling. This seems surprising at first sight, but the same result applies for the 1D t-J chain at the integrable point.[49] Siller *et al.*[22] also found a tiny result for the inverse compressibility of the isotropic t-J ladder near half filling. The result can be understood as follows. The dispersion relation in the conduction band flattens out near the band edge, and hence the dispersion relation of a single hole at half filling is quadratic in momentum q, as illustrated by the free fermion equation (11) or the calculation of Sushkov[26] for the t-J ladder. The dispersion relation for a bound hole-pair bosonic excitation will likewise be quadratic in q. The vanishing of any term linear in q implies that $v_\rho \to 0$ and Eq. (22) then leads to $\kappa^{-1}n^{-2}=0$.

B. Quarter filling

Next we consider states at or near the quarter filling point ($n=1/2$). Reliable results are very hard to obtain for $J_z/t \geqslant 3$. Phase separation presumably occurs in this region, so that the ground state becomes inhomogeneous, and very difficult to treat by DMRG methods. For the most part, our results will be for smaller J_z/t.

1. Odd-even gap

Figure 13 shows the energy gap between states with odd and even numbers of holes, $[E(n_h=L+1,S^z=-1/2)+E(n_h=L-1,S^z=-1/2)-2E(n_h=L,S^z=0)]/2$, where n_h is the number of holes, as a function of J_z/t. It can be seen that for J_z/t less than about 1.3, this gap is small and positive, but for

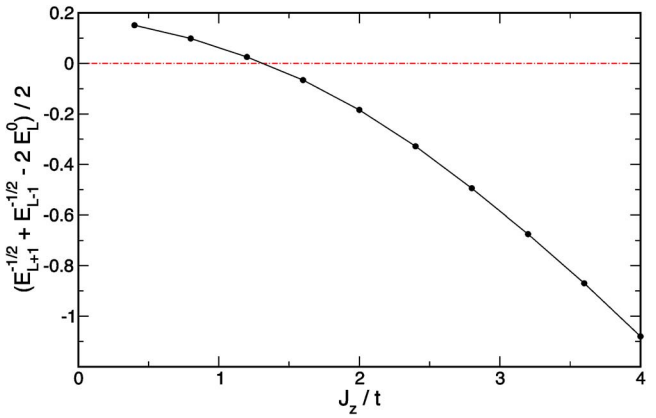

FIG. 13. (Color online) The odd-even gap $[E(n_h=L+1, S^z=-1/2)+E(n_h=L-1, S^z=-1/2)-2E(n_h=L, S^z=0)]/2$ at quarter filling, as a function of J_z/t.

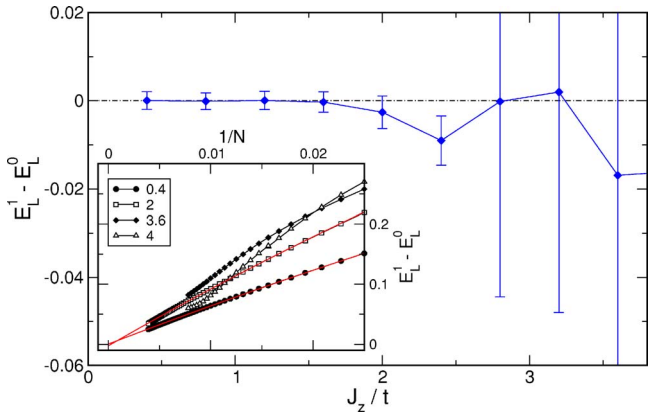

FIG. 14. (Color online) The spin gap $[E(n_h=L,\ S^z=1)-E(n_h=L,\ S^z=0)]$ at quarter filling, as a function of J_z/t.

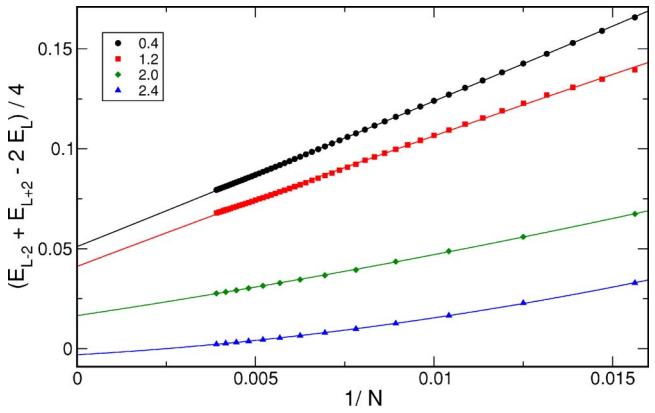

FIG. 15. (Color online) The two-hole gap $[E(n_h=L+2,\ S^z=0)+E(n_h=L-2,\ S^z=0)-2E(n_h=L,\ S^z=0)]/2$ at quarter filling, as a function of $1/N=1/(2L)$, at selected values of J_z/t.

larger J_z/t it is negative. This indicates the absence of any pairing effect between holes in this region.

2. Spin gap

Figure 14 shows the spin gap $[E(n_h=L,S^z=1)-E(n_h=L,S^z=0)]$ as a function of J_z/t. The insert shows examples of the finite-size scaling behavior of this quantity as a function of $1/N$, and the linear extrapolations made to the bulk limit. It can be seen that the results are consistent with zero over the whole region $J_z/t\leqslant 4$. Convergence for $J_z/t>2$ is not very good due to strong finite-size scaling effects (the $J_z/t=4$ case was checked carefully to ensure that the complex scaling is not an artifact of DMRG truncation). Thus for $J_z/t\geqslant 2.3$, we appear to be in the C1S1 phase discussed by Hayward and Poilblanc[12] for the t-J ladder, where both the charge gap and the spin gap vanish.

3. Two-hole gap

Figure 15 shows the two-hole energy gap $[E(n_h=L+2,S^z=0)+E(n_h=L-2,S^z=0)-2E(n_h=L,S^z=0)]$ as a function of $1/N$ at selected values of J_z/t. For $J_z/t\leqslant 2.3$, the gap appears to scale to a finite value in the bulk limit $N\to\infty$, whereas the limit is consistent with zero from there on. Figure 16 shows the estimated bulk limit as a function of J_z/t. The finite charge gap for $J_z/t<2.3$ corresponds to a cusp in the energy density versus filling factor surface, and is evidence of the formation of a CDW state at this commensurate filling factor, according to White *et al.*[23]

We have looked for further evidence of the CDW state in the electron-density profiles and correlation functions. The density profile on an odd-rung lattice at quarter filling shows some evidence of rung-to-rung oscillations, but they die away as $N\to\infty$, and so do not seem to correspond to the CDW.

Examples of the density-density correlation functions are shown in Fig. 17, with one site fixed at the middle of the ladder, and the distance to the other site varying, including both sites on the same leg and those on the opposite leg of the ladder. There is a positive correlation for nearby sites, and a Friedel rung-to-rung oscillation near the boundary. In the intermediate region, there is no strong evidence of either a rung-to-rung alternation or a checkerboard alternation. One major qualitative difference is obvious, however, between Figs. 17(a) and 17(c). At $J_z/t=2$, the correlation function is virtually zero at intermediate and large distances, as one would expect of a solid phase: this is consistent with the CDW behavior. For $J_z/t=3$, on the other hand, the correlation function has a substantial dip at intermediate distances, which actually increases with increasing lattice size. This behavior is more reminiscent of a liquid or a gas.

V. DISCUSSION

As expected, the phase behavior of the t-J_z ladder at $T=0$ appears to be broadly similar to its counterpart, the t-J ladder. A schematic diagram is shown in Fig. 18. At half filling, the system is equivalent to an Ising antiferromagnet, with long-range magnetic order; but at any finite temperature or hole density, the order parameter will vanish, leaving only finite-range antiferromagnetic correlations.

Near half filling, phase separation into hole-rich and hole-poor regions occurs beyond $J_z/t\simeq 4.0$, which is about half the critical value for the t-J_z chain,[32] but twice the critical

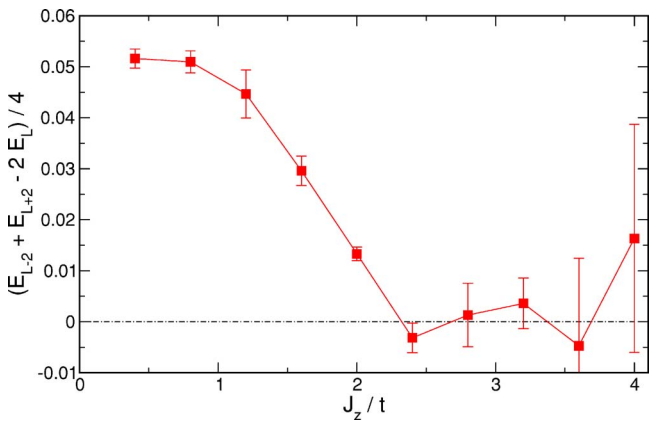

FIG. 16. (Color online) The estimated two-hole gap in the bulk limit $[E(n_h+L+2,\ S^z=0)+E(n_h=L-2,\ S^z=0)-2E(n_h=L,\ S^z=0)]/2$ at quarter filling, as a function of J_z/t.

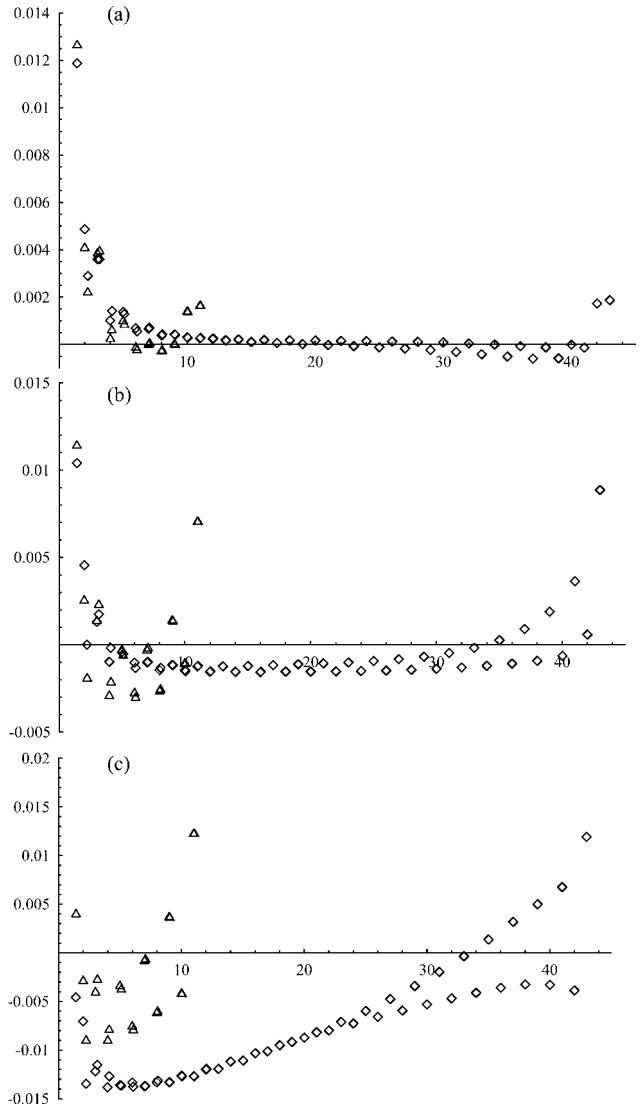

FIG. 17. The density-density correlation function as a function of distance, with one site fixed at the middle of the ladder and the other varying, at quarter filling. Triangles: $L=22$; squares: $L=88$. (a) $J_z/t=2.0$; (b) $J_z/t=2.6$; (c) $J_z/t=3.0$.

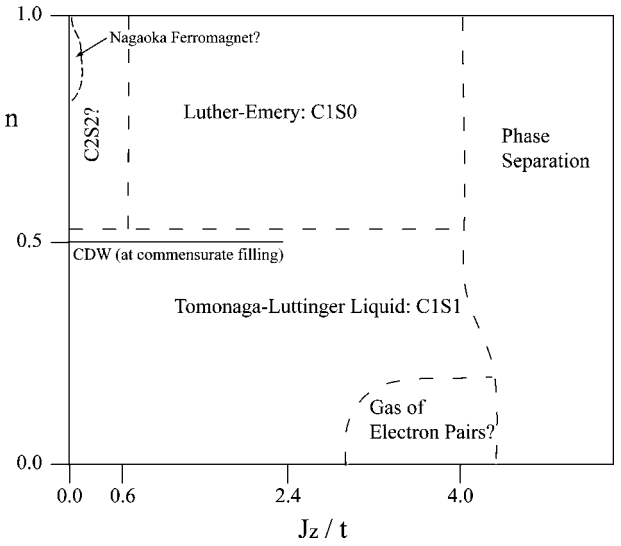

FIG. 18. Schematic phase diagram for the t-J_z ladder.

value for the full t-J ladder.[10] Below that, there is a C1S0 or Luther-Emery phase, where the holes bind into pairs and the charge gap vanishes, but the spin gap remains finite. The spin gap is discontinuous at half filling, because the exciton spin gap is less than the magnon gap. These features are identical with those found for the t-J model.[10] We have not explored the question whether there are superconducting correlations in this region, but they are expected to be present if $K_\rho > 1/2$.

The binding between hole pairs vanishes in the $S^z=1$ channel below $J_z/t \simeq 1.8$, and in the $S^z=0$ channel below $J_z/t \simeq 0.6$. Below that, the holes repel each other, and we presumably enter the C2S2 gapless phase discussed by Müller and Rice[14] for the t-J case (although exact diagonalization data up to $N=14$ are somewhat equivocal as to whether the $S_z=1$ states are degenerate). These different regimes are clearly evident in the hole density profiles on a finite lattice.

In the Nagaoka limit as $J_z/t \to 0$, a finite-lattice calculation reveals rather different behavior in the two models in the one-hole sector. In the t-J case, a state with maximal spin S crosses over the $S=1/2$ state to become the ground state as $J/t \to 0$. For the t-J_z system, on the other hand, the $S^z=1/2$ state remains the ground state at all J_z/t, and the Nagaoka limit is approached smoothly. States with higher S^z become degenerate with the $S^z=1/2$ state in the limit, to form a multiplet with maximum total spin S. Any ferromagnetic correlations in the ground state appear to be transverse to the z direction, as argued by White and Affleck.[41] Our DMRG results for the one-hole gap appear to decrease as $(J_z/t)^{1/2}$, rather than $(J_z/t)^{2/3}$ as predicted by theory; the theory needs re-examination for this case.

Some crude estimates of the effective Hamiltonian parameters in the Luther-Emery phase were made at half filling. Friedel-type fits to the density profiles give $K_\rho \simeq 0.8-1.0$, although it is not clear that the Schulz argument[42] that $K_\rho = 1$ at half filling is applicable to the t-J_z case. We found that $v_\rho = 0$ in that limit, a general result which should apply to chains and ladders for both models.

We have also made some studies of the quarter filled case. For $J_z/t \leqslant 2.3$, the system appears to be in a CDW state, with a finite two-hole gap and solidlike density-density correlation functions, although we could not discover any particular pattern of charge-density waves. This behavior was predicted for a commensurate filling factor by White, Affleck, and Scalapino.[23] We find that the spin gap vanishes in this phase, and in fact is compatible with zero at all couplings. For $J_z/t \geqslant 2.3$, any pairing effects are weak or nonexistent, and the system appears to be in a C1S1 Tomonaga-Luttinger phase with a single gapless spin and single gapless charge

mode, similar to that discussed for the t-J ladder at densities at or below quarter filling by Hayward and Poilblanc.[12] The calculations become very unstable beyond $J_z/t \simeq 3$, and we take this as indicating the onset of phase separation again at larger J_z/t. At very small electron densities, an electron-paired phase should exist. These findings are indicated schematically in Fig. 18.

ACKNOWLEDGMENTS

This work forms part of a research project supported by a grant from the Australian Research Council. We are grateful for extensive computational support provided by the Australian Partnership for Advanced Computing (APAC) National Facility and by the Australian Centre for Advanced Computing and Communications (ac3).

[1] T. M. Rice, Z. Phys. B: Condens. Matter **103**, 165 (1997).
[2] E. Dagotto and T. M. Rice, Science **271**, 618 (1996).
[3] F. D. M. Haldane, Phys. Rev. Lett. **50**, 1153 (1983).
[4] Z. Hiroi and M. Takano, Nature (London) **377**, 41 (1995).
[5] M. Azuma, Z. Hiroi, M. Takano, K. Ishida, and Y. Kitaoka, Phys. Rev. Lett. **73**, 3463 (1994).
[6] P. W. Anderson, Science **235**, 1196 (1987).
[7] F. C. Zhang and T. M. Rice, Phys. Rev. B **37**, 3759 (1988).
[8] E. Dagotto, J. Riera, and D. J. Scalapino, Phys. Rev. B **45**, 5744 (1992).
[9] H. Tsunetsugu, M. Troyer, and T. M. Rice, Phys. Rev. B **49**, 16078 (1994).
[10] M. Troyer, H. Tsunetsugu, and T. M. Rice, Phys. Rev. B **53**, 251 (1996).
[11] D. Poilblanc, D. J. Scalapino, and W. Hanke, Phys. Rev. B **52**, 6796 (1995).
[12] C. A. Hayward and D. Poilblanc, Phys. Rev. B **53**, 11721 (1996).
[13] C. A. Hayward, D. Poilblanc, and D. J. Scalapino, Phys. Rev. B **53**, R8863 (1996).
[14] T. F. A. Müller and T. M. Rice, Phys. Rev. B **58**, 3425 (1998).
[15] J. Riera, D. Poilblanc, and E. Dagotto, Eur. Phys. J. B **7**, 53 (1999).
[16] G. B. Martins, C. Gazza, and E. Dagotto, Phys. Rev. B **62**, 13926 (2000); G. B. Martins, J. C. Xavier, L. Arrachea, and E. Dagotto, *ibid.* **64**, 180513(R) (2001); R. M. Fye, G. B. Martins, and E. Dagotto, *ibid.* **69**, 224507 (2004).
[17] M. Brunner, S. Capponi, F. F. Assaad, and A. Muramatsu, Phys. Rev. B **63**, 180511 (2001).
[18] S. R. White and D. J. Scalapino, Phys. Rev. B **55**, 6504 (1997).
[19] G. Sierra, M. A. Martin-Delgado, J. Dukelsky, S. R. White, and D. J. Scalapino, Phys. Rev. B **57**, 11666 (1998).
[20] G. Sierra, M. A. Martin-Delgado, J. Dukelsky, S. R. White, and D. J. Scalapino, Phys. Rev. B **57**, 11666 (1998).
[21] S. Rommer, S. R. White, and D. J. Scalapino, Phys. Rev. B **61**, 13424 (2000).
[22] T. Siller, M. Troyer, T. M. Rice, and S. R. White, Phys. Rev. B **63**, 195106 (2001).
[23] S. R. White, I. Affleck, and D. J. Scalapino, Phys. Rev. B **65**, 165122 (2002).
[24] U. Schollwock, S. Chakravarty, J. O. Fjaerestad, J. B. Marston, and M. Troyer, Phys. Rev. Lett. **90**, 186401 (2003).
[25] D. Poilblanc, E. Orignac, S. R. White, and S. Capponi, Phys. Rev. B **69**, 220406(R) (2004).
[26] O. P. Sushkov, Phys. Rev. B **60**, 3289 (1999).
[27] M. Sigrist, T. M. Rice, and F. C. Zhang, Phys. Rev. B **49**, 12058 (1994).
[28] Y. L. Lee, Y. W. Lee, C. Y. Mou, and Z. Y. Weng, Phys. Rev. B **60**, 13418 (1999).
[29] W. Zheng and C. J. Hamer, Phys. Rev. B **66**, 085112 (2002).
[30] J. Oitmaa, C. J. Hamer, and Weihong Zheng, Phys. Rev. B **60**, 16364 (1999).
[31] C. Jurecka and W. Brenig, Physica B **312**, 592 (2002).
[32] C. D. Batista and G. Ortiz, Phys. Rev. Lett. **85**, 4755 (2000).
[33] T. Barnes, E. Dagotto, A. Moreo, and E. S. Swanson, Phys. Rev. B **40**, 10977 (1989).
[34] J. Riera and E. Dagotto, Phys. Rev. B **47**, 15346 (1993).
[35] A. L. Chernyshev and P. W. Leung, Phys. Rev. B **60**, 1592 (1999).
[36] J. A. Riera, Phys. Rev. B **64**, 104520 (2001).
[37] Y. Nagaoka, Phys. Rev. **147**, 392 (1966).
[38] W. F. Brinkman and T. M. Rice, Phys. Rev. B **2**, 1324 (1970).
[39] B. I. Shraiman and E. D. Siggia, Phys. Rev. Lett. **60**, 740 (1988).
[40] C. L. Kane, P. A. Lee, and N. Read, Phys. Rev. B **39**, 6880 (1989).
[41] S. R. White and I. Affleck, Phys. Rev. B **64**, 024411 (2001).
[42] H. J. Schulz, Phys. Rev. B **59**, R2471 (1999).
[43] S. R. White, Phys. Rev. Lett. **69**, 2863 (1992); Phys. Rev. B **48**, 10345 (1993).
[44] The figure of $M=60$ refers to the maximum number of states we keep in a given z-spin-charge (S^z,Q) sector of the system block. A reference state is defined in the (S^z,Q) sector with the highest probability—namely the Mth state in that (S^z,Q) sector. All other sectors have their states truncated in a way that is consistent with this reference state, i.e., so that no states are retained that are less probable than the reference state. Hence for a typical profile of states in the various (S^z,Q) sectors the number of states retained in a sector decreases rapidly as we move away from the reference sector in (S^z,Q) space. Thus $M=60$ will correspond to an overall total number of around 300 basis states in the block: see *Density Matrix Renormalization*, edited by I. Peschel, X. Wang, M. Kaulke, and K. Hallberg (Springer, New York, 1999).
[45] G. Martinez and P. Horsch, Phys. Rev. B **44**, 317 (1991).
[46] Z. Liu and E. Manousakis, Phys. Rev. B **45**, 2425 (1992).
[47] C. J. Hamer, W-H. Zheng, and J. Oitmaa, Phys. Rev. B **58**, 15508 (1998).
[48] S. Schmitt-Rink, C. M. Varma, and A. E. Ruckenstein, Phys. Rev. Lett. **60**, 2793 (1988).
[49] M. Ogata, M. U. Luchini, S. Sorella, and F. F. Assaad, Phys. Rev. Lett. **66**, 2388 (1991).